

Removal of Toluene from Nitrogen Gas by Adsorption in a Fixed Bed Column: Experimental and Theoretical Breakthrough Curves

Kaushal Naresh Gupta, Nandagiri Jagannatha Rao, and Govind Kumar Agarwal

Abstract—Experiments were carried out to study adsorption of toluene a volatile organic compound (VOC) on the granular activated carbon. The range of experimental variables studied is as follows: inlet gas concentration (7000 – 11500 ppm), gas flow rate (50 – 70 ml/min) and height of the adsorbent bed (0.015 – 0.025 m). The breakthrough curves were then drawn between ratios of outlet gas concentration to inlet gas concentration versus time for different operating conditions. A mathematical model was developed to predict the VOC breakthrough characteristics on granular activated carbon. The model incorporated the effects of the gas-particle film mass transfer resistance, adsorbent pore diffusion and instantaneous local adsorption equilibrium at the pore surface. The experimental data and the corresponding model simulated results were compared and found to be in good agreement.

Index Terms—Adsorption, Breakthrough Curve, Granular Activated Carbon, Toluene.

I. INTRODUCTION

Rapid economic development and urban population growth have triggered a series of challenges to the endeavors of maintaining the clean air. Urban air quality is cause of public concern, largely as a result of instances of smog and health problems. New pollutants are being increasingly recognized. Air pollution sources have grown and so also the pollutants. Some of these have led to emission of some hazardous air pollutants like volatile organic compounds. Volatile Organic Compounds (VOCs) are chemicals that evaporate easily at room temperature i.e. they have high enough vapor pressure under normal conditions to significantly vaporize and enter the atmosphere. They are characterized by a very high vapor pressure, exceeding 0.5 kPa at 25°C [1]. VOCs are aliphatic and aromatic hydrocarbons, which may contain hetero-atoms, like oxygen, sulphur, nitrogen, halogens. A wide range of carbon based molecules such as aldehydes, ketones, hydrocarbons etc are VOCs. Volatile organic compounds are contributors to the formation of ozone and other photochemical oxidants leading to urban smog. Many VOCs

have been identified as toxic, carcinogenic or mutagenic at concentrations levels found in urban environment [2]. VOC exposures are often associated with an odor while at other times there is no odor. Both can be harmful. Emissions of VOCs originate from breathing and loading losses from storage tanks, venting to process vessels, leaks from piping and equipment [3]. There are thousands of different VOCs produced and used in our daily lives. For e.g. Benzene, Toluene, Methylene chloride, Formaldehyde, Xylene, Ethylene glycol, 1,3-Butadiene etc. Approximately 235 million tons of VOCs are released per year into the atmosphere by man-made sources [4]. The subject has become important because of the impact on environment and human.

Recommended strategies for reducing organic vapors include product substitution or reformulation, thermal or catalytic incineration and activated carbon adsorption (followed by regeneration of the adsorbent and VOC and VOC recovery or catalytic incineration of the highly concentrated stream) [5]. The removal of volatile organic compounds commonly performed by adsorption is of great interest for the air quality control. At a low-concentration level, adsorption on active carbon is the most employed method for the removal of VOCs [6]. The need is an adsorption process is to have a porous solid medium providing high adsorptive capacity. A large surface area or large micro-pore volume can be achieved due to the porous structure of the solid. The breakthrough curve is reflective of the adsorbents performance under dynamic conditions. A relatively larger breakthrough time and gradual increase in the concentration following breakthrough are desirable.

One of the main issues is the concentration measurement of VOC in a gas-vapor mixture. Reference [7] assumed gas to be saturated after being passed through the column filled with the VOC liquid. Reference [8], [9] also assumed the exit gas to be saturated with VOC at the concentration corresponding to the temperature of the bubbler. Reference [10] passed nitrogen gas through two fritted glass bubblers connected in series containing VOC liquid and immersed in a temperature-controlled water bath and then the exit nitrogen gas from the second bubbler was assumed to be saturated with VOC corresponding to the temperature of the bubbler. Reference [11] also prepared a gas-vapor mixture by the passage of nitrogen through a saturator containing chlorobenzene at 0°C and then the exit gas was assumed to be saturated. Hence by reviewing the literature it has been found that in most of the studies carried so far on the adsorption of VOCs the concentration of VOC in the gas-vapor mixture was found by assuming it as saturated gas after being passed through VOC liquid. In such techniques it

Manuscript received August 11, 2011; revised September 19, 2011.

Kaushal Naresh Gupta is with the Department of Chemical Engineering, Jaypee University of Engineering & Technology, Guna- 473226, India. (Tel.: +91-7544-267310, fax: +91-7544-267011, e-mail: kaushalnaresh74@gmail.com.)

Nandagiri Jagannatha Rao is with Jaypee University of Engineering & Technology, Guna-473226, India. (e-mail: nj.rao@juet.ac.in)

Govind Kumar Agarwal is with the Department of Chemical Engineering, Jaypee University of Engineering & Technology, Guna-473226, India. (e-mail: gk.agarwal@juet.ac.in)

is always debatable whether the vapor-gas mixture is saturated or not. In the present study the technique used for measuring the concentration of VOC in a gas-vapor mixture was by drawing a calibration curve obtained from the saturated gas-vapor mixture prepared separately in a gas collector at a particular fixed temperature.

The major objectives of this study were as follows: (1) set-up of an experimental test bench to study the adsorption phenomena for the removal of VOCs by commercially available granular activated carbon, (2) obtain breakthrough curves under varying operating conditions such as inlet concentrations, gas flow rate and height of the adsorbent bed and (3) development of a mathematical model to understand the adsorption mechanism and predict the breakthrough profiles.

II. MATHEMATICAL MODELING

In this section, a mathematical model is presented to predict the time-dependent (unsteady state) concentration profiles of the adsorbing species (VOCs) on a solid adsorbent under isothermal conditions. One important point that may be noted is that, in reality the steady-state condition never exists in the bed of adsorbing materials during adsorption. Hence, a finite adsorption rate always prevails in the bed. The steady- state is achieved only when the bed reaches saturation levels. The present mathematical model takes account of both external and internal mass transfer resistances as well as of non- ideal plug flow along the column. Simultaneously, instantaneous local adsorption equilibrium on the pore surface is considered [12]. The following assumptions are made in theoretical analysis for developing a mathematical model for the adsorption of VOCs on granular activated carbon.

- (i) The system operates under isothermal conditions.
- (ii) Intraparticle mass transport is due to Fickian diffusion, and is characterized by D_e . Mass transfer across the boundary layer surrounding the solid particles is characterized by the external-film mass transfer coefficient k_m .
- (iii) Axial dispersion is considered to account for non-ideal flux along the longitudinal axis of the column.
- (iv) The macroporous adsorbent particles are spherical and homogeneous in size and density.

The present model is based on three governing equations: (a) species balance of the adsorbing component in the bed, (b) species balance of the component inside the pores of the adsorbent, and (c) instantaneous local adsorption equilibrium at the pore surface.

Based on the preceding assumptions, the mass balance of the adsorbing component in a cross-section of the column yields:

$$\varepsilon_b \frac{\partial C_b}{\partial t} + \varepsilon_b V_z \frac{\partial C_b}{\partial z} - \varepsilon_b D_L \frac{\partial^2 C_b}{\partial z^2} = -\frac{3(1-\varepsilon_b)}{R_p} k_m (C_b - C_{ps}) \quad (1)$$

where ε_b is the bed porosity.

C_b is the solute concentration in the bulk gas phase in kg/m^3 .

C_{bo} is the initial concentration of solute in the gas phase in kg/m^3 .

V_z is the velocity in m/s.

D_L is the axial dispersion coefficient in m^2/s .

R_p is the radius of the adsorbent particle in m.

k_m is the external-film mass-transfer coefficient in m/s.

C_{ps} is the solute concentration at the external surface of the adsorbent particle in kg/m^3 .

Boundary conditions:

$$\text{at } t = 0, \quad C_b = 0 \text{ at all } z$$

$$\text{at } t > 0, z = 0 \quad C_b = C_{bo}$$

$$z = L, \quad \frac{\partial C_b}{\partial z} = 0$$

where L is the length of the fixed bed in m.

In non-dimensional form (1) reduces to (2):

$$C_b^* = \frac{C_b}{C_{bo}}$$

$$z^* = \frac{z}{L}$$

$$C_{ps}^* = \frac{C_{ps}}{C_{bo}}$$

$$\frac{\partial C_b^*}{\partial t} = -\frac{1}{t_{res}} \frac{\partial C_b^*}{\partial z^*} + P \frac{\partial^2 C_b^*}{\partial z^{*2}} - Q(C_b^* - C_{ps}^*) \quad (2)$$

where $t_{res} = \frac{L}{V_z}$, $P = \frac{D_L}{L^2}$ and $Q = \frac{3k_m}{R_p} \frac{1-\varepsilon_b}{\varepsilon_b}$

Non-dimensional boundary conditions:

$$\text{at } t = 0, \text{ and at all } z^*, \quad C_b^* = 0$$

$$\text{at } t > 0, \text{ and at } z^* = 0, \quad C_b^* = 1$$

$$z^* = 1, \quad \frac{\partial C_b^*}{\partial z^*} = 0$$

The intra-pellet mass transfer is due to the diffusion of adsorbate molecules through the pore. Hence the mass balance of the adsorbing component inside the pores of the adsorbent is given by:

$$\alpha \frac{\partial C_p}{\partial t} + (1-\alpha) \rho \frac{\partial q}{\partial t} = D_p \left(\frac{\partial^2 C_p}{\partial r^2} + \frac{2}{r} \frac{\partial C_p}{\partial r} \right) \quad (3)$$

where α is the particle porosity.

C_p is the solute concentration in the gaseous phase inside the pores in kg/m^3 .

ρ is the particle density in kg/m^3 .

q is the solute concentration on the adsorbed phase in kg/kg .

D_e is the effective diffusivity in m^2/s .

Assuming instantaneous equilibrium

$$\frac{\partial q}{\partial t} = \frac{\partial C_p}{\partial t} \frac{\partial q}{\partial C_p} \quad (4)$$

Assuming Langmuir isotherm,

$$q = \frac{q_m K C_p}{1 + K C_p} \quad (5)$$

Here q_m is the maximum adsorption capacity of the adsorbent in kg/kg and K is the langmuir isotherm constant in m^3/kg .

Substituting (4) and (5) in (3), we get

$$\frac{\partial C_p}{\partial t} = \left[\frac{1}{1 + \rho \left(\frac{1-\alpha}{\alpha} \right) \frac{q_m K}{(1 + K C_p)^2}} \right] D_e \left(\frac{\partial^2 C_p}{\partial r^2} + \frac{2}{r} \frac{\partial C_p}{\partial r} \right) \quad (6)$$

Boundary conditions:

$$C_p = 0 \text{ at } t = 0$$

$$\frac{\partial C_p}{\partial r} = 0 \text{ at } r = 0$$

$$D_e \frac{\partial C_p}{\partial r} = k_m (C_b - C_{ps}) \text{ at } r = R_p$$

In non-dimensional form (6) reduces to (7):

$$C_p^* = \frac{C_p}{C_{bo}}$$

$$r^* = \frac{r}{R_p}$$

$$\frac{\partial C_p^*}{\partial t} = \frac{T \alpha (1 + K C_{bo} C_p^*)^2}{\alpha (1 + K C_{bo} C_p^*)^2 + \rho (1 - \alpha) q_m K} \left[\frac{\partial^2 C_p^*}{\partial r^{*2}} + \frac{2}{r^*} \frac{\partial C_p^*}{\partial r^*} \right] \quad (7)$$

$$\text{where } T = \frac{D_e}{R_p^2}$$

Non-dimensional boundary conditions:

$$C_p^* = 0 \text{ at } t^* = 0$$

$$\frac{\partial C_p^*}{\partial r^*} = 0 \text{ at } r^* = 0$$

$$\frac{\partial C_p^*}{\partial r^*} = R (C_b^* - C_{ps}^*) \text{ at } r^* = 1 \text{ where } R = \frac{k_m R_p}{D_e}$$

Here q_m and K are langmuir isotherm parameters, which are usually obtained from the experimental adsorption data under equilibrium conditions. For the model simulation, q_m and K were used as adjusted parameter models for predicting the breakthrough curves under varying conditions.

A. Numerical solution technique

Since nonlinear adsorption equilibrium is considered, the preceding set of partial differential equations (2) & (7) were solved numerically by a reduction to a set of ordinary differential equations using the orthogonal collocation method [13], [14]. Equation (2) was discretized in 14 collocation points including the boundary point and (7) was discretized in 8 collocation points including the boundary point. The solution of this set of coupled equations was

performed by a mathematical algorithm, developed in MATLAB (v.7.1) software, implemented into a computer program. The program used the ODE15s solver from MATLAB that applies the variable order, variable step Gear method. On a Pentium IV machine the CPU time of computation was found to be less than a minute.

III. EXPERIMENTAL STUDIES

The experiments were carried on granular activated carbon (density 400 kg/m^3) particles of diameter 1.5 mm and of density 400 kg/m^3 . The other physical properties of activated carbon were found from [15] and are listed in Table I. The several operating conditions under which the adsorption experiments were carried out were inlet concentration of VOC, gas flow rate and adsorbent bed height. Table II describes these conditions.

TABLE I: PHYSICAL PROPERTIES OF ACTIVATED CARBON [15]

Parameter	Unit	Range
BET surface area	m^2/g	1100 – 1200
Particle porosity	-	0.4 – 0.6
Macropore volume	cm^3/g	0.2 – 0.5
Micropore volume	cm^3/g	0.15 – 0.5

TABLE II: RANGE OF EXPERIMENTAL VARIABLES

Parameter	Unit	Range
Inlet VOC concentration	ppm	7000-11500
Gas flow rate	ml/min	50-70
Weight of adsorbent	g	4 – 6.63
Bed height	m	0.015 – 0.025
Adsorption temperature	K	304

A. Experimental Set - up

Fig.1 is the schematic of the experimental set-up designed and used for carrying out adsorption experiments. The set-up consists of three sections: a gas preparation section, an adsorption section, and an analytical section. In the gas preparation section, carrier gas (nitrogen in this case) is bubbled in the liquid VOC (i.e. toluene) contained in a vertical glass column (0.7 m long and 0.05 m diameter). Isothermal conditions are maintained in the column by circulating water at a fixed temperature around the column. The bubbler is made of SS of 6.35 mm diameter tube whose bottom end is closed and the outer surface is perforated with a hole of diameter 0.08 mm near the bottom and nitrogen is bubbled in the toluene liquid through the hole. Part of the nitrogen gas at a measured flow rate is bubbled through the toluene liquid and another part of nitrogen is sent directly to the mixing chamber for getting the desired dilution. The

resulting gas-vapor mixture from the mixing chamber is sent to the adsorption section consisting of a vertical glass column (I.D = 5 cm, L= 10 cm) filled with an adsorbent with provisions for the gas inlet and outlet. The effluent gas stream from the adsorption section is passed to the analytical section consisting of a gas chromatograph (MICHRO-9100, Netel (India) limited) with flame ionization detector (FID) and data station. A computer is connected to the data station to store the peak area. There is a provision of a by-pass line for measuring the inlet concentration of toluene through gas chromatograph.

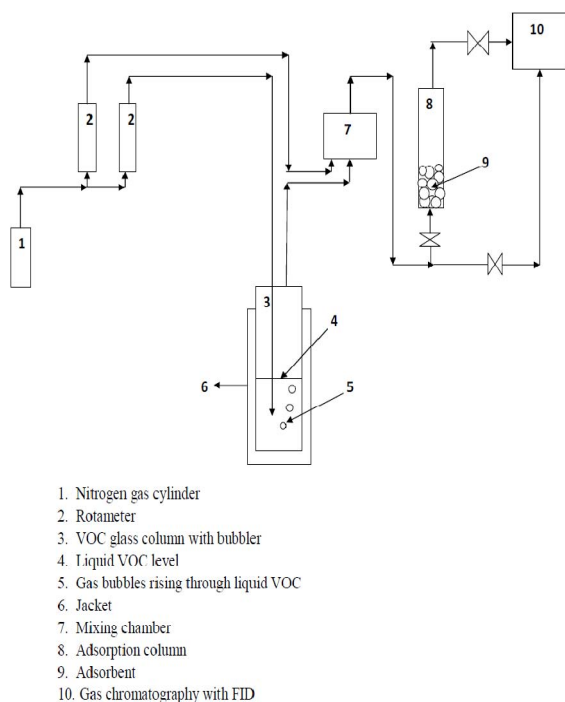


Fig. 1 Schematic diagram of the experimental set-up for VOC adsorption.

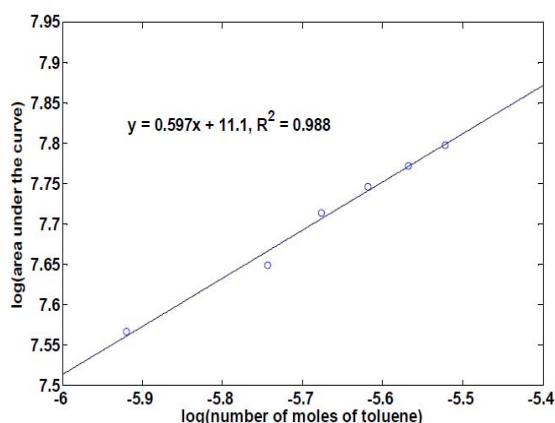


Fig. 2 Calibration curve for toluene concentration in a gas stream

B. Experimental Procedure

A calibration curve is drawn for measuring the concentration of toluene vapor in a gas-vapor mixture. First a saturated mixture of gas containing toluene vapor is prepared. It is prepared in a gas collector which is partially filled with toluene liquid and then purged with nitrogen gas to remove last traces of air. Then it is kept in an oven maintained at a constant temperature of 313 K for 5-6 hours so that nitrogen gas in the vapor space gets saturated with toluene vapor. Then different volumes of samples are

collected through septum fitted in gas collector with a gas-tight syringe from a vapor space and inserted it in a GC. A calibration curve shown in Fig.2 is then drawn between log of number of moles of toluene in the sample and log of area under the curve obtained from the GC to get a straight line. This calibration curve is used further in this study for finding out the concentration of toluene in unknown gas-vapor mixture.

Prior to start of the experiments the glass column was filled with a VOC liquid up to a certain height for getting the desired concentration of VOC in a gas-vapor mixture. Water was circulated at a fixed temperature around the column and a sufficient time was given (1 hour) to attain the required temperature. The weighed amount of granular activated carbon was placed into the adsorption column and is supported by glass wool from both sides to avoid any carryover of adsorbent particles. Nitrogen gas at a measured flow rate is bubbled through VOC liquid and also it was sent directly to the mixing chamber for dilution at a fixed flow rate. The concentration of the inlet gaseous mixture is measured by GC prior to the start of the adsorption process. It takes around 3 – 4 hours for the inlet gas to reach the steady state and then this gaseous mixture was allowed to pass through the adsorption column. As the adsorption process is started, the transient concentrations of exit gas from the adsorption column (breakthrough data) are monitored and measured by GC. Breakthrough curves are then drawn for different operating conditions. In each case breakthrough time is found out which is defined as time taken for the effluent concentration to reach 5% of the inlet concentration.

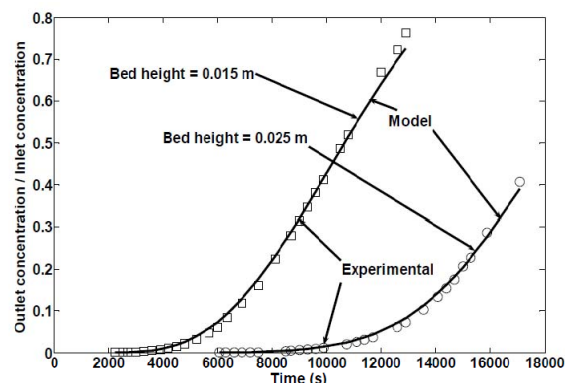


Fig. 3 Effect of bed height on breakthrough curve (Gas flow rate = 70 ml/min, Inlet concentration = 11500 ppm, particle diameter = 0.0015 m).

IV. RESULTS AND DISCUSSION

A. Effect of Bed Height

To determine the effects of bed height on the breakthrough characteristics, the experiments were carried out for varying bed heights: 0.015 and 0.025 m. For each run the inlet gas concentration was maintained at 11500 ppm and the gas flow rate was set at 70 ml/min. Fig. 3 describes the experimentally obtained breakthrough curves for toluene under the various bed heights. As observed from Fig. 3, the breakthrough time increases from 5747 to 12174 seconds as the bed height is increased from 0.015 to 0.025 m. The increase in the breakthrough time with increase in the bed height as observed from Fig.4 can be explained in terms of the total amount of adsorbent present in the bed. With

increase in the bed height which implies more amount of adsorbent under identical flow rates and inlet gas concentrations the bed will get saturated in a longer time.

Fig.3 also shows that the model predictions agree well with the experimental data. For the model predictions of the breakthrough curves under identical experimental conditions, the values of q_m and K were to be adjusted. The corresponding values of q_m and K obtained are reported in Table III.

TABLE III VALUES OF ADJUSTABLE PARAMETERS FOR VARIOUS BED HEIGHTS (INLET VOC CONCENTRATION = 11500 PPM, GAS FLOW RATE = 70 ML/MIN)

Parameter	Bed height = 0.015 m	Bed height = 0.025 m
q_m (kg/kg)	0.117	0.114
K (m ³ /kg)	35.574	35.787

B. Effect of Inlet VOC Concentration

To determine the effects of inlet VOC concentration on the breakthrough characteristics, the experiments were carried out for varying VOC inlet concentrations: 7000 and 11500 ppm. For each run 4 g of the adsorbent was taken and the gas flow rate was set at 70 ml/min. Fig. 4 describes the experimentally obtained breakthrough curves for toluene under the various gas inlet concentrations. As observed from Fig. 4, the breakthrough time decreases from 6187 to 5747 seconds as the inlet concentration is increased from 7000 to 11500 ppm. The increase in the breakthrough time with the decrease in the inlet concentration levels as observed from Fig.4 can be explained in terms of the total amount of VOC. With decrease in the inlet concentration under identical flow rates, the total amount of VOC (moles) entering the macropores of the adsorbent is less. Therefore, the saturation of the adsorbent bed is delayed and occurs in relatively longer time.

Fig.4 also shows that the model predictions agree well with the experimental data. Again for the model predictions of the breakthrough curves under identical experimental conditions, the values of q_m and K were to be adjusted. The corresponding values of q_m and K obtained are reported in Table IV.

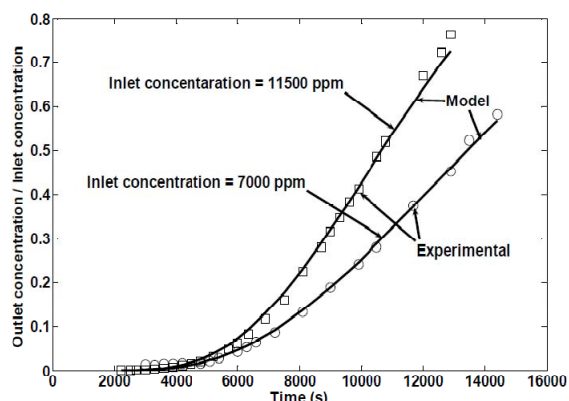


Fig. 4 Effect of inlet concentration on breakthrough curve (Gas flow rate = 70 ml/min, bed height = 0.015 m, particle diameter = 0.0015 m).

TABLE IV VALUES OF ADJUSTABLE PARAMETERS FOR VARIOUS INLET GAS CONCENTRATIONS (GAS FLOW RATE = 70 ML/MIN, BED HEIGHT = 0.015 M)

Parameter	Inlet gas concentration = 7000 ppm	Inlet gas concentration = 11500 ppm
q_m (kg/kg)	0.116	0.117
K (m ³ /kg)	35.645	35.574

C. Simulation Studies

It has been found from Table III and Table IV that the values of adjustable parameters q_m and K to explain the experimental data are almost same. Hence for further simulations q_m and K are selected to be 0.117 kg/kg and 35.574 m³/kg respectively. Here simulations have been carried out in order to find out the effects of some variables like flow rate and particle diameter on breakthrough curve which could not be found out experimentally. The effect of flow rate could not be found out experimentally in the present set-up because to maintain a constant inlet concentration VOC liquid level in the column had to be changed which required hit and trial method. Hence its effect is predicted through simulation of adsorption column. The diameter of the adsorbent particle used in all experiments is 1.5 mm. Hence the effect of different diameter of the adsorbent particles on breakthrough curves can also be predicted through simulation of adsorption column. The effect of pore diffusivity on breakthrough curves can be also be found out. The various parameters used in simulations studies such as Re , Sc , Pe , mass transfer coefficient; k_m , axial dispersion coefficient; D_L , effective diffusivity, D_e are reported in Table V. The values of k_m , D_L and D_e , are found from the reported correlations [16] (refer Appendix).

TABLE V CALCULATED VALUES OF Re , Sc , Pe , D_L , K_m AND D_e UNDER VARIOUS OPERATING CONDITIONS

S.NO	Q (ml/min)	D_p , m	$V_z \times 10^3$, m/s	Re	Sc	Pe	$D_L \times 10^8$, m ² /s	k_m , m/s	$D_e \times 10^8$, m ² /s
1.	40	0.0015	3.397	0.0383	1.478	0.1886	10.57	0.0131	1.7797
2.	70	0.0015	5.944	0.057	1.478	0.3291	6.061	0.0135	1.7797
3.	100	0.0015	8.492	0.0958	1.478	0.4682	4.2612	0.0138	1.7797
4.	70	0.001	5.944	0.0446	1.478	0.2199	6.0475	0.0197	1.7797
5.	70	0.002	5.944	0.0893	1.478	0.4374	6.081	0.0103	1.7797
6.	400	0.0015	33.9	0.383	1.478	1.6824	1.1857	0.0162	1.7797

D. Effect of Gas Flow Rate

As observed from Fig.5 both the breakthrough time and the total adsorption time decrease with increase in flow rate. Here the breakthrough time has decreased from 11500 to 3114 seconds as the gas flow rate is increased from 40 to 100 ml/min. This is due to the increase in mass transfer coefficient with the increase in gas flow rate resulting in the increase in adsorption rate, due to which the bed will get saturated in a shorter time.

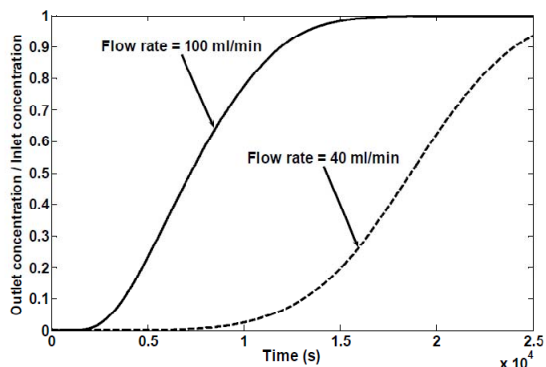


Fig. 5 Effect of gas flow rate on breakthrough curve (Inlet concentration = 11500 ppm, bed height = 0.015 m, particle diameter = 0.0015 m).

E. Effect of Particle Diameter

As observed from the Fig.6, decrease in the particle size from 0.002 m to 0.001 m resulted in significant increase in breakthrough time from 3695 to 7862 seconds. The noticeable characteristic of the breakthrough responses, especially for the small size particles is the abrupt increase in the concentration levels following the break-through of the bed due to which time for bed saturation decreases. The decrease in breakthrough time in case of large size particles is attributed due to the longer diffusion path in the pores. However the time of bed saturation increases due to the large adsorption surface area of the particle. Pre-determining such type of breakthrough characteristic of an adsorbing material is important for selecting the particle size.

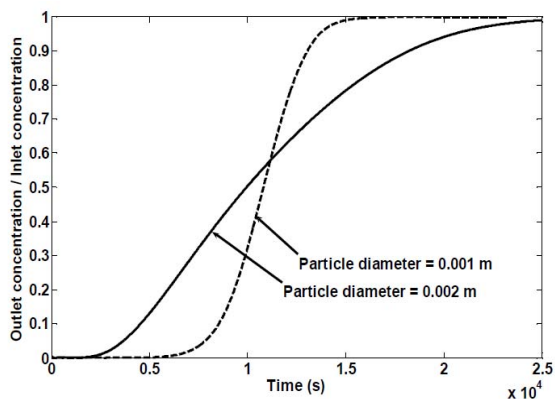


Fig. 6 Effect of particle diameter on breakthrough curve (Inlet concentration = 11500 ppm, bed height = 0.015 m, gas flow rate = 70 ml/min).

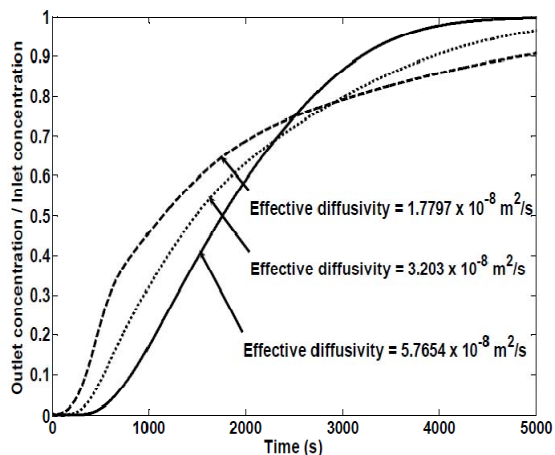


Fig. 7 Effect of pore diffusivity on breakthrough curve (gas flow rate = 400 ml/min).

F. Effect of Pore Diffusivity

The pore size of an adsorbent is a critical parameter in determining the breakthrough characteristics of an adsorbate. Smaller is the pore size, larger is the diffusion time of adsorbing species within the pores due to relatively smaller diffusivity. The larger diffusion time causes the adsorption process to be diffusion limited. In order to determine the conditions under which pore diffusion becomes limiting in adsorption of VOC, simulations have been carried out for varying effective diffusivity and gas flow rates.

Fig.7 and Fig.8 describe the effect of pore diffusivity on breakthrough curves. In the former, a gas flow rate of 400 ml/min has been chosen, while in the later a lower flow rate, 40 ml/min is chosen keeping the remaining operating variables identical. As shown in Fig.7, at a flow rate of 400 ml/min, the adsorption rates are significantly altered by variation in diffusivity, D_e . On the other hand, at a lower gas flow rate (40 ml/min) the adsorption rate is found to remain unaffected over large values of D_e as shown in Fig.8.

From the above simulation results, the following conclusions can be drawn: (a) in general, the effect of pore diffusivity on adsorption rate is significant at high flow rates; implying adsorption process is limited by pore diffusion, and (b) the effect of pore diffusivity on adsorption rate is almost negligible at low flow rates; implying the gas-particle film mass transfer controls the adsorption process.

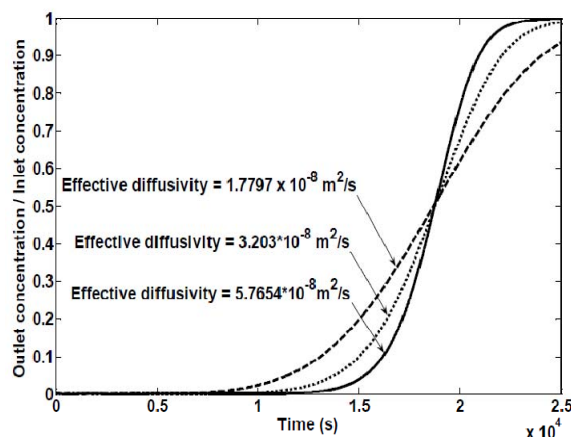


Fig. 8 Effect of pore diffusivity on breakthrough curve (gas flow rate = 40ml/min).

V. CONCLUSIONS

The adsorption of toluene on granular activated carbon has been studied for various operating parameters. The breakthrough time increased with increase in bed height and it decreased with increase in inlet concentration. Furthermore, a mathematical model accounting for external-film and pore-diffusion mass-transfer mechanisms, axial dispersion and nonlinear isotherm was used to fit the experimental breakthrough curves. The model reproduced adequately the experimental results once the best-fitting parameters were attained. Then the effect of gas flow rate, particle diameter and pore diffusivity on breakthrough curves were predicted through the developed mathematical model. It was found that at low gas flow rates gas-particle film mass-transfer controls the overall adsorption process

while at higher gas flow rates it is the pore diffusivity which controls the overall adsorption process.

APPENDIX

1. The axial dispersion co-efficient in the packed bed, D_L is expressed in terms of Peclet number defined as, $Pe = 2R_p\mu/D_L\rho_g$. The Peclet numbers are correlated with particles Reynolds and Schmidt numbers through one of the empirical correlations as follows [16]:

$$\frac{1}{Pe} = \frac{0.3}{Re \times Sc} + \frac{0.5}{1 + 3.8/(Re \times Sc)}$$

for $0.008 < Re < 400$ and $0.28 < Sc < 2.2$

where μ is the viscosity of the gas in kg/m.s and ρ_g is the gas density in kg/m³.

2. The mass transfer co-efficient k_m in the packed bed is calculated using the following correlation for Sherwood number as, $Sh = 2k_mR_p/D_m$ [16]:

$$Sh = 2 + 1.1(Sc)^{0.33}(Re)^{0.6}$$

where D_m is the molecular diffusivity in m²/s.

3. The effective diffusivity inside the pores is determined by using the formula:

$$D_e = \frac{D\alpha}{\tau}$$

Here τ is the tortuosity factor and its value generally lies between 2 to 6 [17]. In this study, an average value of 4 has been taken. The combined diffusivity, D inside the pores is given by a combination of both Knudsen (D_k) and molecular (D_m) diffusivities as:

$$\frac{1}{D} = \frac{1}{D_k} + \frac{1}{D_m}$$

where Knudsen diffusivity is given as:

$$D_k = 97 \times r_{pore} \sqrt{\frac{T}{M}}$$

Here r_{pore} is the pore radius in m, M is the molecular weight of a VOC in kg/kmol and T is the temperature in K.

REFERENCES

- [1] M. Magureanu, N.B. Mandache, P. Eloy, E.M. Gaigneaux, V.I. Parvulescu, "Plasma-assisted catalysis for volatile organic compounds abatement", Applied catalysis B: Environmental, 61, 2005, pp.12-20.
- [2] A. Srivastava, "Source apportionment of ambient VOCs in Mumbai city", Atmospheric Environment, 38, 2004, pp. 6829-43.
- [3] F.I. Khan, A.K. Ghoshal, "Removal of volatile organic compounds from polluted air", Journal of Loss Prevention in the Process Industries, 13, 2000, pp. 527-45.
- [4] A.O. Malley, B.K. Hodnett, "The influence of volatile organic compound structure on conditions required for total oxidation", Catalysis Today, 54, 1999, pp. 31-38.
- [5] A.B. Fuertes, G. Marban, D.M. Nevskaja, "Adsorption of volatile organic compounds by means of activated carbon fibre-based monoliths", Carbon, 41, 2003, pp. 87-96.
- [6] G. Marban, T.V. Solis, A. B. Fuertes, "Modeling the breakthrough behavior of an activated carbon fiber monolith in n-butane adsorption from diluted streams", Chemical Engineering Science, 61, 2006, pp. 4762-72.
- [7] D. Das, V. Gaur, N. Verma, "Removal of volatile organic compound by activated carbon fiber", Carbon, 42, 2004, pp. 2949-62.
- [8] P. Dwivedi, V. Gaur, A. Sharma, N. Verma, "Comparative study of removal of volatile organic compounds by cryogenic condensation and adsorption by activated carbon fiber, Separation and Purification Technology, 39, 2004, pp. 23-37.
- [9] V.Gaur, A. Sharma, N.Verma, "Catalytic oxidation of toluene and m-xylene by activated carbon fiber impregnated with transition metals", Carbon, 43, 2005, pp. 3041-53.
- [10] M. Lordgoei, K.R. Carmichael, T.W. Kelly, M. J. Rood, S. M. Larson, "Activated carbon cloth adsorption-cryogenic system to recover toxic volatile organic compounds", Gas. Sep. Purif., 10, 1996, pp. 123-30.
- [11] L.Asnin, A.Fedorov, D.Yakusheva, "Adsorption of chlorobenzene vapor on V2O5/Al2O3 catalyst under dynamic conditions", Adsorption, 14, 2008, pp. 771-79.
- [12] L.F. Bautista, M. Martinez, J. Aracil, "Adsorption of α -Amylase in a Fixed Bed: Operational efficiency and Kinetic Modeling", AIChE Journal, 49, 2003, pp. 2631-41.
- [13] S.Pon, "Polynomial Approximation Techniques for differential equations in electrochemical problems in 'Electroanalytical chemistry'", Bard, A.J., Editor, Mariel Dekker Inc., New York, 1984.
- [14] S.K. Gupta, "Numerical Methods for Engineers", New Age International publishers, 2010.
- [15] D.M. Ruthven, "Principles of adsorption and adsorption processes", John Wiley & Sons, New York, 1984, pp.8.
- [16] R.T. Yang, "Gas separation by Adsorption Processes", Imperial College Press, UK, 1997.
- [17] L.I. Xiang, L.I. Zhong, Luo Ling'ai, "Adsorption kinetics of dibenzofuran in activated carbon packed bed", Chinese Journal of Chemical Engineering, 16, 2008, pp. 203-208.